ELSEVIER

Journal of Power Sources 93 (2001) 186–200

JOURNAL OF POWER SOURCES

www.elsevier.com/locate/jpowsour

Resistive companion battery modeling for electric circuit simulations

B. Wu[a], R. Dougal[b], R.E. White[a,*]

[a]Department of Chemical Engineering, University of South Carolina, Columbia, SC 29208, USA
[b]Department of Electrical Engineering, University of South Carolina, Columbia, SC 29208, USA

Received 7 August 2000; accepted 27 August 2000

Abstract

Resistive companion (RC) modeling is an easy-to-use approach for electric circuit simulations. With a RC numerical solver, simulations of complex electric systems can be achieved based on RC models. In this study, the construction of RC battery models is investigated. A general battery model and a nickel–metal hydride cell model have been built. Simulations of RC battery models on virtual test bed (VTB) are presented and analyzed. It is shown that RC modeling provides a flexible and powerful way for the simulation of battery systems.

Keywords: Battery modeling; Battery simulation; Electric circuit simulation; Resistive companion modeling; Virtual test bed

1. Introduction

Battery becomes more and more important in our life with the growing popularity of portable electric devices, e.g. camera, cellular phone, and laptop, etc. Some high-energy batteries (e.g. lithium ion battery and nickel–metal hydride battery) are under active research at present, which hopefully will lead to some breakthroughs in the power storage techniques in the future. Due to the complex chemical and physical processes involved, the behavior of battery is usually harder to predict compared with that of electric and mechanic devices [1]. A widely used battery model is described by the following equation

$$E = E_0 + IR_{\text{int}} \tag{1}$$

In the above equation, it is assumed that a battery has a constant open-circuit potential and the potential of a loaded battery varies linearly with the applied current. This model is actually oversimplified, i.e. it cannot reflect many characteristics of a real battery, such as only limited amount of energy is available from a battery, and the open-circuit potential of a battery changes with the state of charge (SOC), etc. Hence, it cannot be used in serious simulations.

First-principle battery modeling becomes popular in recent years. It is an effective approach for battery design and optimization. Since detailed chemical and physical processes are considered, first-principle battery models are generally complicated (with a large set of differential/algebraic equations and tens or hundreds of parameters). As a result, these models require significant computational power and cannot be integrated easily with other simulation programs to investigate the behavior of whole power systems. In fact, most first-principle battery models in literature are coded in Fortran for standalone simulations and are usable for only limited operations.

Circuit simulation has been widely used in the electrical engineering field. There are many circuit simulation programs available today, e.g. widely used SPICE [2]. Recently, a heavily funded project, virtual test bed (VTB), provides another choice of electric circuit simulation programs (downloadable from http://web.engr.sc.edu/vtb/). VTB was originally designed to simulate an electric ship. Later on, it was expanded to provide more capabilities to simulate general engineering systems, e.g. hybrid electric vehicles. VTB has two major components: design environment and visualization engine. The first component (see Fig. 1) provides a visual design platform and performs numerical calculations. The second component (see Fig. 2) accepts the results from the first component and presents them in dynamic plots. A comprehensive library of models has been developed for VTB, which permits simulation of many engineering systems. Detailed information about the VTB project can be found on the VTB web site.

After a system has been designed in the VTB environment, the numerical solver of VTB utilizes the information contained in the worksheet and the resistive companion (RC) models of the relevant devices to predict the dynamic

* Corresponding author. Tel.: +1-803-777-3270; fax: +1-803-777-8265.
E-mail address: white@engr.sc.edu (R.E. White).

0378-7753/01/$ – see front matter
PII: S0378-7753(00)00574-7

Nomenclature

a_{neg}	specific surface area of the negative electrode (cm^2/cm^3)
a_{pos}	specific surface area of the positive electrode (cm^2/cm^3)
A_{neg}	geometry area of the negative electrode (cm^2)
A_{pos}	geometry area of the positive electrode (cm^2)
b	equivalent current source of an electric device (A)
$\boldsymbol{B}$	current source vector (A)
c_e	concentration of KOH electrolyte (mol/cm^3)
$c_{e,ref}$	reference concentration of KOH electrolyte (mol/cm^3)
c_{MH}	concentration of hydrogen in metal hydride (mol/cm^3)
$c_{MH,max}$	maximum concentration of hydrogen in metal hydride (mol/cm^3)
$c_{MH,ref}$	reference concentration of hydrogen in metal hydride (mol/cm^3)
$c_{Ni(OH)_2}$	concentration of $Ni(OH)_2$ (mol/cm^3)
$c_{Ni(OH)_2,max}$	maximum concentration of $Ni(OH)_2$ (mol/cm^3)
$c_{Ni(OH)_2,ref}$	reference concentration of $Ni(OH)_2$ (mol/cm^3)
C_{bat}	capacity of the battery (A h)
E	potential of a loaded battery (V)
E_0	standard potential of a battery (V)
E_{eq}	open-circuit potential of a battery at a particular state of charge (V)
$\boldsymbol{f}$	linear or nonlinear equations
F	Faradic constant (98467 C/eq)
$\boldsymbol{F}$	governing equations of voltage variables
g	equivalent conductance of an electric device (S)
$\boldsymbol{G}$	conductance matrix (S)
i	current through an electric device (A)
$\boldsymbol{i}$	vector of current (A)
$i_{4,ref}$	rate of oxygen reaction at the reference state (A/cm^2)
i_{cell}	current through a cell (A)
i_k	current on terminal k (A)
$i_{o,k}$	exchange current density of reaction k (A/cm^2)
j_1	current density due to the nickel reaction on the positive electrode (A/cm^2)
j_2	current density due to the oxygen reaction on the positive electrode (A/cm^2)
j_3	current density due to the hydrogen reaction on the negative electrode (A/cm^2)
j_4	current density due to the oxygen reaction on the negative electrode (A/cm^2)
$\boldsymbol{J}$	Jacobian matrix with respect to voltage variables
l_{neg}	thickness of the metal hydride electrode (cm)
l_{pos}	thickness of the nickel electrode (cm)
$l_{y,neg}$	equivalent thickness of metal hydride material (cm)
$l_{y,pos}$	equivalent thickness of nickel active material (cm)
$\boldsymbol{L}$	lower triangular matrix
L_{MH}	loading of metal hydride material (g/cm^2)
$L_{Ni(OH)_2}$	loading of nickel active material (g/cm^2)
$\boldsymbol{m}$	temporary vector in matrix manipulation
M_{MH}	molecular weight of metal hydride material (g/mol)
$M_{Ni(OH)_2}$	molecular weight of nickel active material (g/mol)
n	electron transfer number of the whole battery reaction
p_{O_2}	pressure of oxygen (atm)
$p_{O_2,ref}$	reference pressure of oxygen (atm)
R	ideal gas constant (8.3143 J/mol/K)
R_{int}	internal resistance of a battery (Ω)
SOC	state of charge of the battery
t	independent time variable (s)
T	temperature (K)
$\boldsymbol{u}$	vector of independent control variables
$\boldsymbol{U}$	upper triangular matrix
$U_{eq,k,ref}$	equilibrium potential of reaction k at reference reactant concentrations (V)
v	voltage across an electric device (V)
$\boldsymbol{v}$	vector of voltages (V)
v_{cell}	voltage through a cell (V)
v_k	voltage on terminal k (V)
V_{gas}	gas volume in a nickel–metal hydride cell (cm^3)
$\boldsymbol{y}$	vector of internal state variables

Greek letters

Δi_{cell}	change of current due to the perturbation of the voltage (A)
Δv_{cell}	perturbation of the voltage (V)
$\Delta\phi_{neg}$	potential different at the solid–liquid interface on the negative electrode (V)
$\Delta\phi_{pos}$	potential different at the solid–liquid interface on the positive electrode (V)
$\phi_{neg,l}$	potential in the liquid phase on the negative electrode (V)
$\phi_{neg,s}$	potential in the solid phase on the negative electrode (V)
$\phi_{pos,l}$	potential in the liquid phase on the positive electrode (V)
$\phi_{pos,s}$	potential in the solid phase on the positive electrode (V)
ρ_{MH}	density of metal hydride active material (g/cm^3)
$\rho_{Ni(OH)_2}$	density of nickel active material (g/cm^3)

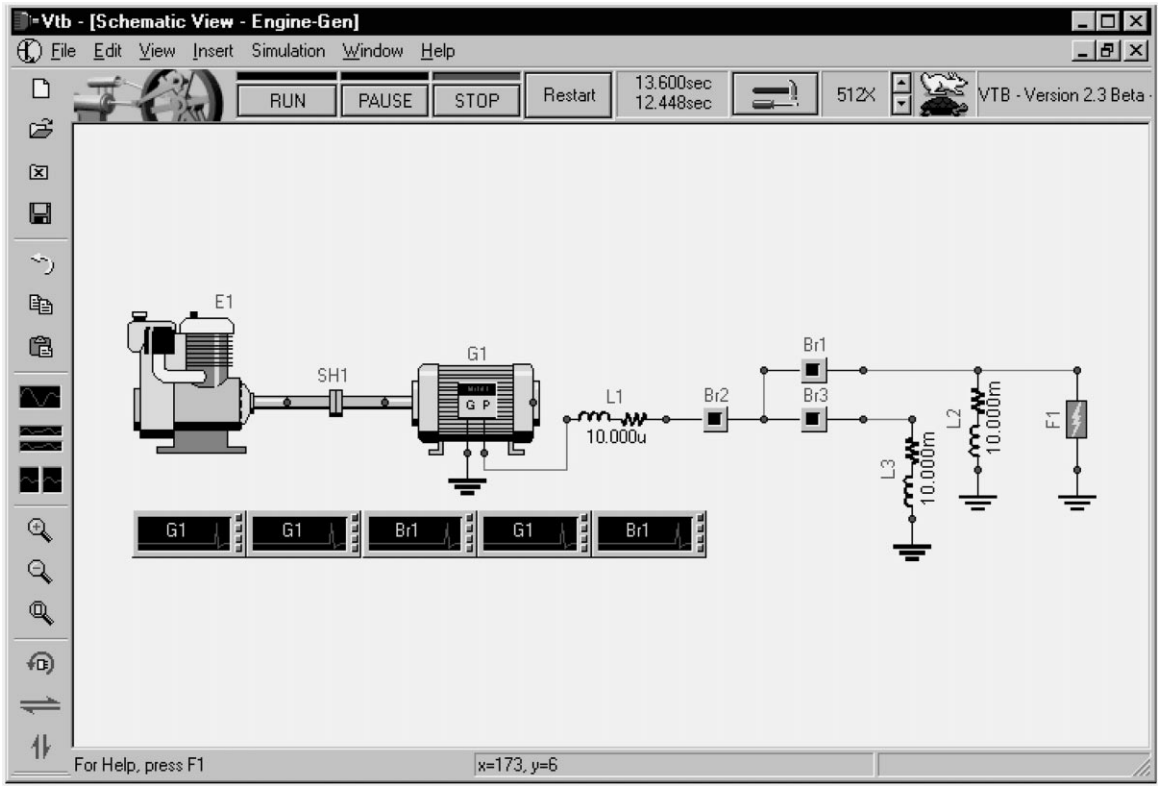

Fig. 1. The VTB design environment.

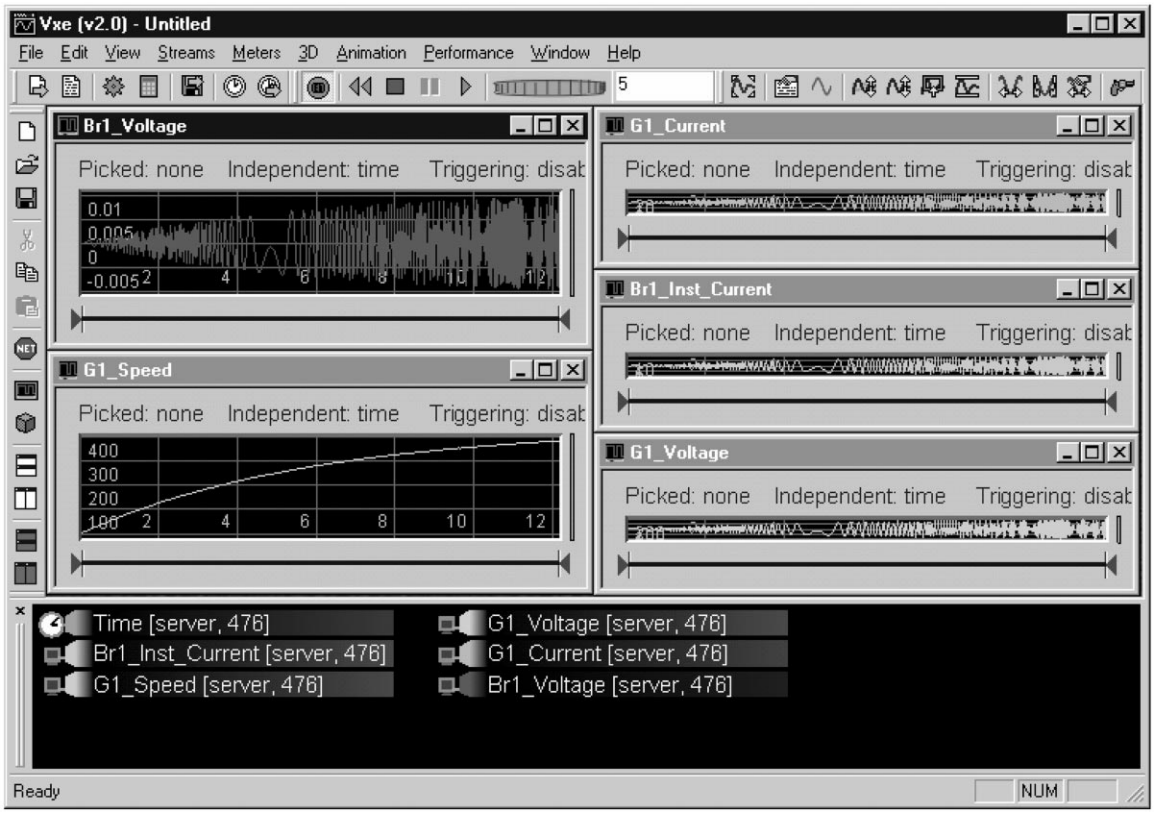

Fig. 2. The VTB visualization engine.

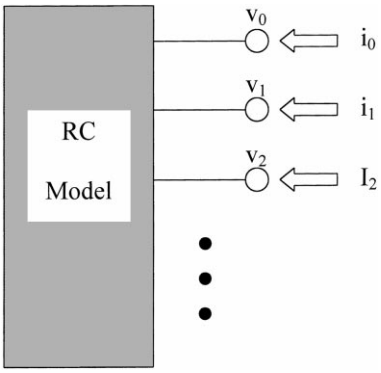

Fig. 3. RC black box model of an electric device.

behavior of the system. For each electric device, a black box RC model with some external terminals (see Fig. 3) [3] can be used to describe its electric behavior. The governing equations of the device are cast in the following form

$$\begin{bmatrix} \boldsymbol{i} \\ \boldsymbol{0} \end{bmatrix} = \begin{bmatrix} \boldsymbol{f}_1(\dot{\boldsymbol{v}}, \dot{\boldsymbol{y}}, \boldsymbol{v}, \boldsymbol{y}, \boldsymbol{u}) \\ \boldsymbol{f}_2(\dot{\boldsymbol{v}}, \dot{\boldsymbol{y}}, \boldsymbol{v}, \boldsymbol{y}, \boldsymbol{u}) \end{bmatrix} \tag{2}$$

where $\boldsymbol{v}$ is the vector of terminal voltages, $\boldsymbol{i}$ the vector of terminal currents, $\boldsymbol{y}$ the vector of internal state variables and $\boldsymbol{u}$ the vector of independent control variables.

A linear form of Eq. (2) is used by VTB, as given below

$$\begin{bmatrix} \boldsymbol{i}(t) \\ \boldsymbol{0} \end{bmatrix} = \begin{bmatrix} \boldsymbol{G}_{11}(t)\boldsymbol{v}(t) + \boldsymbol{G}_{12}(t)\boldsymbol{y}(t) - \boldsymbol{B}_1(t) \\ \boldsymbol{G}_{21}(t)\boldsymbol{v}(t) + \boldsymbol{G}_{22}(t)\boldsymbol{y}(t) - \boldsymbol{B}_2(t) \end{bmatrix} \tag{3}$$

where $\boldsymbol{G}$ is the conductance matrix and $\boldsymbol{B}$ the current source vector. For a nonlinear device, Eq. (3) is obtained by linearizing the nonlinear governing equations with the Taylor series expansion.

The RC modeling approach essentially treats each electric device as a system of conductors and current sources. A RC model accepts the values of terminal voltages as input and calculates the conductance matrix and the current source vector as output. A dynamic RC model also needs to conduct the integration of the differential equations for a specified time step. Each RC model only handles its own governing equations. The RC numerical solver of VTB will take care of the solving of all interconnected devices in a system. For a dynamic system, at each time step the RC solver adjusts the voltages of all connecting nodes in the electric circuit based on the previous values until the numerical convergence is achieved, i.e. the sum of incoming currents is approximately zero at all connecting nodes. A summary of the algorithm used by the RC solver is provided in the Appendix A, which is essentially a nonlinear equation solving procedure based on Newton's algorithm. More details can be found in the studies by Cokkinides and Beker [3].

2. RC modeling of batteries

Battery is a typical electric device with the input/output of current and voltage. In fact, it can be treated as a nonlinear source device with two terminals, as shown in Fig. 4. For a two-terminal electric device, RC modeling expects the following relation

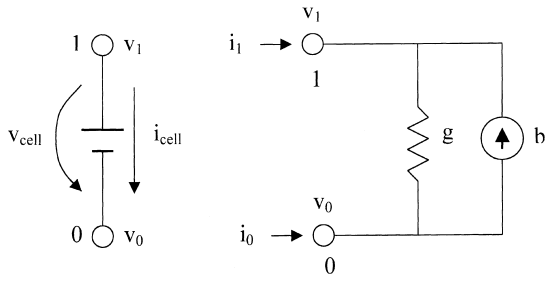

Fig. 4. Diagram of a battery RC model where $v_{\text{cell}} = v_1 - v_0$ and $i_{\text{cell}} = i_1 = -i_0$. The matrices b and g are given in Eqs. (5) and (6).

$$i = gv - b \tag{4}$$

The conductance is given by

$$g = \frac{\mathrm{d}i}{\mathrm{d}v} \tag{5}$$

The current source is calculated by

$$b = gv - i \tag{6}$$

Put the relations among dependent variables into RC matrix form, we have

$$\boldsymbol{I} = \boldsymbol{G}\boldsymbol{V} - \boldsymbol{B} \tag{7}$$

where

$$\boldsymbol{V} = \begin{bmatrix} v_0 \\ v_1 \end{bmatrix} \tag{8}$$

$$\boldsymbol{I} = \begin{bmatrix} i_0 \\ i_1 \end{bmatrix} \tag{9}$$

$$\boldsymbol{G} = \begin{bmatrix} g & -g \\ -g & g \end{bmatrix} \tag{10}$$

$$\boldsymbol{B} = \begin{bmatrix} -b \\ b \end{bmatrix} \tag{11}$$

The behavior of a battery is usually described in a set of nonlinear equations (for dynamic equations, discretization in time domain is needed) as given below

$$\boldsymbol{f}(v, i, \boldsymbol{y}) = 0 \tag{12}$$

where $\boldsymbol{y}$ is a vector of state variables. To provide a RC battery model, the conductance matrix and the current source vector must be obtained from the governing equations of the battery. Two battery models are presented subsequently to demonstrate the details of the RC modeling approach.

2.1. A simple RC model for general batteries

A simple battery model was developed as an extension of the widely used model Eq. (1). The governing equations of

the model is given by

$$v = E_{eq} + iR_{int} \tag{13}$$

where the equilibrium potential of the battery is a function of the SOC of the battery and can be fitted directly from the experimental data

$$E_{eq} = f(\mathrm{SOC}) \tag{14}$$

If the following assumptions are valid: (i) the Nernst equation is a valid description of the equilibrium potential of the relevant electrochemical reactions; (ii) the main electrochemical reactions on positive and negative electrodes have fast kinetics; (iii) the capacity of the positive electrode roughly matches that of the negative electrode (i.e. no precharge and surplus capacity on either electrode), we have

$$E_{eq} = E_0 + \frac{RT}{nF}\ln\left(\frac{\mathrm{SOC}}{1-\mathrm{SOC}}\right) \tag{15}$$

Assuming no side reactions, then the relationship between SOC and charge/discharge rate is given by

$$\frac{\mathrm{dSOC}}{\mathrm{d}t} = \frac{i}{3600C_{bat}} \tag{16}$$

The equivalent conductance and current source of the model are calculated as follows

$$g = \frac{\mathrm{d}i}{\mathrm{d}v} = \frac{1}{R_{int}} \tag{17}$$

$$b = gv - i = \frac{E_{eq}}{R_{int}} \tag{18}$$

In matrix form, we have the RC model for general batteries.

$$\boldsymbol{I} = \boldsymbol{G}\boldsymbol{V} - \boldsymbol{B} \tag{19}$$

where

$$\boldsymbol{G} = \begin{bmatrix} \dfrac{1}{R_{int}} & -\dfrac{1}{R_{int}} \\ -\dfrac{1}{R_{int}} & \dfrac{1}{R_{int}} \end{bmatrix} \tag{20}$$

$$\boldsymbol{B} = \begin{bmatrix} -\dfrac{E_{eq}}{R_{int}} \\ \dfrac{E_{eq}}{R_{int}} \end{bmatrix} \tag{21}$$

The above battery model is actually a linear model between current and voltage. Due to its simplicity, computational requirement of the model is trivial. This model is more realistic than Eq. (1) and can give reasonable predictions for many battery systems. However, it is still oversimplified. First-principle modeling is needed to obtain more accurate predictions and get mechanistic information of a battery. An example is presented below for a nickel–metal hydride cell.

2.2. RC model of a nickel–metal hydride cell

The model presented here uses the planar electrode approximation for both positive and negative electrodes, i.e. each electrode is treated as a huge planar electrode with a surface area equal to the total internal surface area of the porous electrode. The diffusion process inside the solid active material has been neglected. Since battery electrodes are normally made to be very thin to minimize ohmic resistance, a planar electrode model usually gives insignificant errors and costs much less computation compared with a rigorous porous electrode model.

Four reactions in a nickel–metal hydride cell have been considered (the hydrogen oxidation reaction on the nickel electrode has been neglected), as listed below

- Nickel electrode
  - $\mathrm{NiOOH + H_2O + } e^- \underset{\text{charge}}{\overset{\text{discharge}}{\rightleftarrows}} \mathrm{Ni(OH)_2 + OH^-}$ (22)
  - $\mathrm{2OH^- \rightarrow \tfrac{1}{2}O_2 + H_2O} + 2e^-$ (23)
- Metal hydride electrode
  - $\mathrm{MH + OH^-} \underset{\text{charge}}{\overset{\text{discharge}}{\rightleftarrows}} \mathrm{H_2O + M} + e^-$ (24)
  - $\mathrm{\tfrac{1}{2}O_2 + H_2O} + 2e^- \rightarrow \mathrm{2OH^-}$ (25)

The main reaction on the positive electrode is the redox reaction of nickel active material Eq. (22) while that on the negative electrode is the redox reaction of metal hydride material Eq. (24). The side reaction on the positive electrode is oxygen evolution Eq. (23) while that on the metal hydride electrode is oxygen reduction Eq. (25).

The kinetics of reactions Eqs. (22)–(24) can be described with the Butler–Volmer equation

$$j_1 = i_{0,1}\begin{bmatrix} \left(\dfrac{c_{\mathrm{Ni(OH)_2}}}{c_{\mathrm{Ni(OH)_2,ref}}}\right)\left(\dfrac{c_e}{c_{e,ref}}\right)\exp\left(\dfrac{0.5F}{RT}(\Delta\phi_{pos} - U_{eq,1,ref})\right) \\ -\left(1-\dfrac{c_{\mathrm{Ni(OH)_2}}}{c_{\mathrm{Ni(OH)_2,ref}}}\right)\exp\left(-\dfrac{0.5F}{RT}(\Delta\phi_{pos} - U_{eq,1,ref})\right) \end{bmatrix} \tag{26}$$

$$j_2 = i_{0,2}\begin{bmatrix} \left(\dfrac{c_e}{c_{e,ref}}\right)^2\exp\left(\dfrac{F}{RT}(\Delta\phi_{pos} - U_{eq,2,ref})\right) \\ -\left(\dfrac{p_{O_2}}{p_{O_2,ref}}\right)^{0.5}\exp\left(-\dfrac{F}{RT}(\Delta\phi_{pos} - U_{eq,2,ref})\right) \end{bmatrix} \tag{27}$$

$$j_3 = i_{0,3}\begin{bmatrix} \left(\dfrac{c_{MH}}{c_{MH,ref}}\right)\left(\dfrac{c_e}{c_{e,ref}}\right)\exp\left(\dfrac{0.5F}{RT}(\Delta\phi_{neg} - U_{eq,3,ref})\right) \\ -\exp\left(-\dfrac{0.5F}{RT}(\Delta\phi_{neg} - U_{eq,3,ref})\right) \end{bmatrix} \tag{28}$$

where the potential difference at the solid–liquid interface on each electrode is

$$\Delta\phi_{\text{pos}} = \phi_{\text{pos,s}} - \phi_{\text{pos,l}} \tag{29}$$

$$\Delta\phi_{\text{neg}} = \phi_{\text{neg,s}} - \phi_{\text{neg,l}} \tag{30}$$

Due to the huge electrochemical driving force for oxygen reduction on the negative electrode, a limiting-current equation is used for the rate of reaction Eq. (25)

$$j_4 = -\frac{p_{\text{O}_2}}{p_{\text{O}_2,\text{ref}}} i_{4,\text{ref}} \tag{31}$$

The charge balances on the electrodes is described by

$$i_{\text{cell}} = a_{\text{pos}} l_{\text{pos}} A_{\text{pos}} (j_1 + j_2) \tag{32}$$

$$-i_{\text{cell}} = a_{\text{neg}} l_{\text{neg}} A_{\text{neg}} (j_3 + j_4) \tag{33}$$

The mass balances of nickel active material is given by

$$l_{y,\text{pos}} \frac{\text{d}c_{\text{Ni(OH)}_2}}{\text{d}t} = -\frac{j_1}{F} \tag{34}$$

where the effective thickness of nickel active material is

$$l_{y,\text{pos}} = \frac{L_{\text{Ni(OH)}_2}}{\rho_{\text{Ni(OH)}_2} l_{\text{pos}} a_{\text{pos}}} \tag{35}$$

The mass balance of metal hydride material is given by

$$l_{y,\text{neg}} \frac{\text{d}c_{\text{MH}}}{\text{d}t} = -\frac{j_4}{F} \tag{36}$$

where the effective thickness of metal hydride active material is

$$l_{y,\text{neg}} = \frac{L_{\text{MH}}}{\rho_{\text{MH}} l_{\text{neg}} a_{\text{neg}}} \tag{37}$$

The mass balance equation of oxygen is given by

$$\frac{V_{\text{gas}}}{RT} \frac{\text{d}p_{\text{O}_2}}{\text{d}t} = \frac{(a_{\text{pos}} l_{\text{pos}} A_{\text{pos}} j_2 + a_{\text{neg}} l_{\text{neg}} A_{\text{neg}} j_4)}{F} \tag{38}$$

The separator is treated as an ohmic resistance, which gives

$$i_{\text{cell}} R_{\text{int}} = \phi_{\text{pos,l}} - \phi_{\text{neg,l}} \tag{39}$$

The cell potential is calculated by

$$v_{\text{cell}} = \phi_{\text{pos,s}} - \phi_{\text{neg,s}} = \Delta\phi_{\text{pos}} - \Delta\phi_{\text{neg}} + i_{\text{cell}} R_{\text{int}} \tag{40}$$

Due to the comparatively excess amount of metal hydride material, the SOC of a nickel–metal hydride cell is given by the charged state of nickel active material

$$\text{SOC} = 1 - \frac{c_{\text{Ni(OH)}_2}}{c_{\text{Ni(OH)}_2,\text{max}}} \tag{41}$$

The initial setting of SOC for the model will be converted into corresponding concentration of nickel active material and metal hydride material, i.e.

$$\frac{c^0_{\text{Ni(OH)}_2}}{c_{\text{Ni(OH)}_2,\text{max}}} = 1 - \text{SOC}^0 \tag{42}$$

$$\frac{c^0_{\text{MH}}}{c_{\text{MH,max}}} = \text{SOC}^0 \frac{L_{\text{Ni(OH)}_2} A_{\text{pos}} M_{\text{MH}}}{L_{\text{MH}} A_{\text{neg}} M_{\text{Ni(OH)}_2}} + 0.05 \tag{43}$$

In Eq. (43) metal hydride material has been set to be five percent precharged

For an applied voltage v_{cell} and an integration time step Δt, six dependent variables: i_{cell}, $c_{\text{Ni(OH)}_2}$, c_{MH}, p_{O_2}, $\Delta\phi_{\text{pos}}$ and $\Delta\phi_{\text{neg}}$ need to be solved with the model. Applying the implicit Euler method on the model equations yields

$$l_{y,\text{pos}} \frac{c^{(\text{new})}_{\text{Ni(OH)}_2} - c^{(\text{old})}_{\text{Ni(OH)}_2}}{\Delta t} = -\frac{j^{(\text{new})}_1}{F} \tag{44}$$

$$l_{y,\text{neg}} \frac{c^{(\text{new})}_{\text{MH}} - c^{(\text{old})}_{\text{MH}}}{\Delta t} = -\frac{j^{(\text{new})}_3}{F} \tag{45}$$

$$\frac{V_{\text{gas}}}{RT} \frac{p^{(\text{new})}_{\text{O}_2} - p^{(\text{old})}_{\text{O}_2}}{\Delta t} = \frac{(a_{\text{pos}} l_{\text{pos}} A_{\text{pos}} j^{(\text{new})}_2 + a_{\text{neg}} l_{\text{neg}} A_{\text{neg}} j^{(\text{new})}_4)}{F} \tag{46}$$

$$i^{(\text{new})}_{\text{cell}} = a_{\text{pos}} l_{\text{pos}} A_{\text{pos}} (j^{(\text{new})}_1 + j^{(\text{new})}_2) \tag{47}$$

$$-i^{(\text{new})}_{\text{cell}} = a_{\text{neg}} l_{\text{neg}} A_{\text{neg}} (j^{(\text{new})}_3 + j^{(\text{new})}_4) \tag{48}$$

$$v^{(\text{new})}_{\text{cell}} = \Delta\phi^{(\text{new})}_{\text{pos}} - \Delta\phi^{(\text{new})}_{\text{neg}} + i^{(\text{new})}_{\text{cell}} R_{\text{int}} \tag{49}$$

where the superscript '(old)' indicates the previous values and superscript '(new)' the current values. It is worth noting that the old values of algebraic variables i_{cell}, $\Delta\phi_{\text{pos}}$ and $\Delta\phi_{\text{neg}}$ have no effect on the solution of the current values of dependent variables because no time derivatives of these variables appear in the governing equations. The above equations, which can be written in the form of Eq. (12), are solved with the nonlinear equation solver, general nonlinear equation solver (GNES) [4].

Analytical solutions for the RC matrices are not available for the above model. The equivalent conductance g and current source b of the RC battery model are obtained by using finite difference approximations. That is, g is calculated by a finite difference approximation for $\text{d}i/\text{d}v$ in Eq. (5). This approximation is obtained by first setting v_{cell} followed by calculating i_{cell} and the other dependent variables listed above by solving Eqs. (44)–(49). Next, a small voltage Δv_{cell} is added to v_{cell} and the calculation is repeated to obtain $i_{\text{cell}} + \Delta i_{\text{cell}}$. These values are used to give g and b

$$g = \frac{(i_{\text{cell}} + \Delta i_{\text{cell}}) - i_{\text{cell}}}{(v_{\text{cell}} + \Delta v_{\text{cell}}) - v_{\text{cell}}} \tag{50}$$

$$b = g v_{\text{cell}} - i_{\text{cell}} = \frac{(i_{\text{cell}} + \Delta i_{\text{cell}}) - i_{\text{cell}}}{(v_{\text{cell}} + \Delta v_{\text{cell}}) - v_{\text{cell}}} v_{\text{cell}} - i_{\text{cell}} \tag{51}$$

In matrix form, we have the RC model of the nickel–metal hydride cell as follows

$$\boldsymbol{I} = \boldsymbol{G}\boldsymbol{V} - \boldsymbol{B} \tag{52}$$

where

$$\boldsymbol{G} = \begin{bmatrix} \dfrac{(i_{\text{cell}} + \Delta i_{\text{cell}}) - i_{\text{cell}}}{(v_{\text{cell}} + \Delta v_{\text{cell}}) - v_{\text{cell}}} & -\dfrac{(i_{\text{cell}} + \Delta i_{\text{cell}}) - i_{\text{cell}}}{(v_{\text{cell}} + \Delta v_{\text{cell}}) - v_{\text{cell}}} \\ -\dfrac{(i_{\text{cell}} + \Delta i_{\text{cell}}) - i_{\text{cell}}}{(v_{\text{cell}} + \Delta v_{\text{cell}}) - v_{\text{cell}}} & \dfrac{(i_{\text{cell}} + \Delta i_{\text{cell}}) - i_{\text{cell}}}{(v_{\text{cell}} + \Delta v_{\text{cell}}) - v_{\text{cell}}} \end{bmatrix} \tag{53}$$

$$\boldsymbol{B} = \begin{bmatrix} -\dfrac{(i_{\text{cell}} + \Delta i_{\text{cell}}) - i_{\text{cell}}}{(v_{\text{cell}} + \Delta v_{\text{cell}}) - v_{\text{cell}}} v_{\text{cell}} + i_{\text{cell}} \\ \dfrac{(i_{\text{cell}} + \Delta i_{\text{cell}}) - i_{\text{cell}}}{(v_{\text{cell}} + \Delta v_{\text{cell}}) - v_{\text{cell}}} v_{\text{cell}} - i_{\text{cell}} \end{bmatrix} \tag{54}$$

The perturbation of the cell voltage Δv_{cell} must be small enough (e.g. 1×10^{-4} V) to provide accurate numerical approximations for $\boldsymbol{G}$ and $\boldsymbol{B}$. The numerical approximation of RC matrices essentially allows more complex battery models to be treated as a linear model between current and voltage at a specific time point.

Good efficiency and robustness are highly desirable for a first-principle RC battery model. It is obvious that even with the planar electrode approximation, the first-principle model of a nickel–metal hydride cell is highly nonlinear and nontrivial to solve. In the simulation of a whole power system, since a battery model may be called hundreds or even thousand times by the RC solver, a slow model could cause a simulation to last several days, which will be intolerable for most projects. Normally, simplified models and good numerical solvers should be used to achieve satisfactory calculation efficiency. In the RC approach, the input to a battery models is terminal voltage values; however, the behavior of a battery is highly sensitive to the applied voltages, as is obvious from the exponential dependence of battery current on the voltage values in Eqs. (26)–(28). Some guess values from the RC solver can easily lead to numerical difficulty of a battery model. Thus a RC battery model needs to be built robust enough to avoid numerical failures of the whole simulation.

3. Results and discussions

To incorporate a RC model into VTB, a dynamic link library (DLL) file needs to be constructed based on the C++ interface specified by Cokkinides and Beker [3]. The DLL file of a RC model can be debugged independently. VTB will accept and use the DLL file of a user-built RC model as it does with native RC models. Communication between a RC model and the VTB is through the exchange of model parameters and RC matrices. Sample source code has been provided by Cokkinides and Beker [3] to facilitate the construction of RC models for the VTB environment. A C++ class of a battery model is derived from the base class CCompanionDevice. The following subroutines need to be defined (supposing BatModel is the name of our battery model class):

- BatModel::BatModel(), defines model parameters and states;
- BatModel::GuiToInternal(), converts user settings to internal model parameters;
- BatModel::GetVectorIcon(short* vicondata), provides the icon of the model;

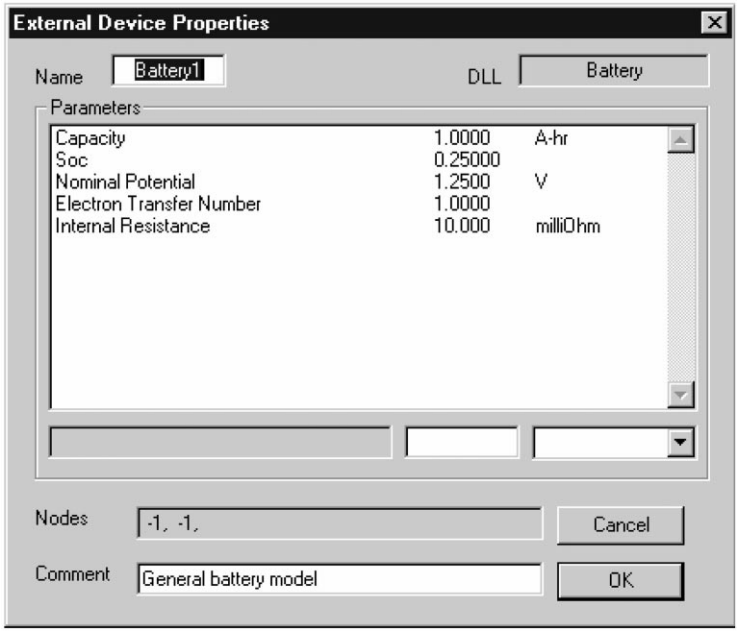

Fig. 5. The parameter setting dialog for the simple RC model of general batteries.

Table 1
Parameters for the simplified model of general batteries

Parameter	Value
C_{bat} (A h)	1.0
E_0 (V)	1.25
n	1.0
R_{int} (Ω)	1.0×10^{-2}

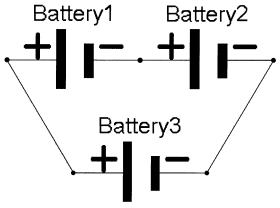

Fig. 6. Worksheet of sample simulation I: two batteries with initial SOC of 25% connected with a battery with initial SOC of 85%.

- BatModel::TdsInitExt(DEV_INTERFACE* tdsi, double* vol, double* beq, double** con), initializes model states and provides VTB with initial RC matrices;
- BatModel::TdsStepExt(DEV_INTERFACE* tdsi), calculates the model states and RC matrices based on the voltage input from VTB RC solver.

After the DLL of a RC model has been developed, it needs to be put into a specified directory to be accepted by VTB. Using a RC model is straightforward in VTB. To create a model object, one selects the corresponding model item from menus or toolbars. The model object is represented by an icon and can be moved around in the VTB worksheet. The parameters of an object can be easily modified through a dialog box (see Fig. 5) invoked by double-clicking the icon of the object.

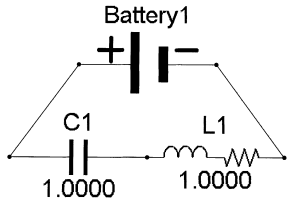

Fig. 8. Worksheet of sample simulation II: a capacitor and an inductor connected in series with a battery with initial SOC of 95%.

Two simulations are given for the simple RC model of general batteries. The parameters of the battery model are listed in Table 1. In Fig. 6, three batteries are connected together. The SOCs of the first two batteries are set to be 25%, and the SOC of the third one is set to be 85%. However, as shown in Fig. 7, it is predicted that two less charged batteries connected in series can actually produce a voltage high enough to charge a near fully charged battery in 15 s, which is quite an unintuitive result (and a fact in reality). In Fig. 8, a battery with an initial SOC of 95% is connected with a 1C capacitor and a 1H inductor. The simulation results in Figs. 9 and 10 show fast transient behavior of voltage and current. The capacitor is charged while the battery is discharged at first. When the capacitor is near fully charged, the current in the circuit approaches zero (the capacitor is essentially open-circuit after fully charged) and the battery voltage approaches the open circuit potential of the battery. Since the battery discharge process only lasts for 10 s, the SOC of the battery only slightly decreases, as shown in Fig. 11.

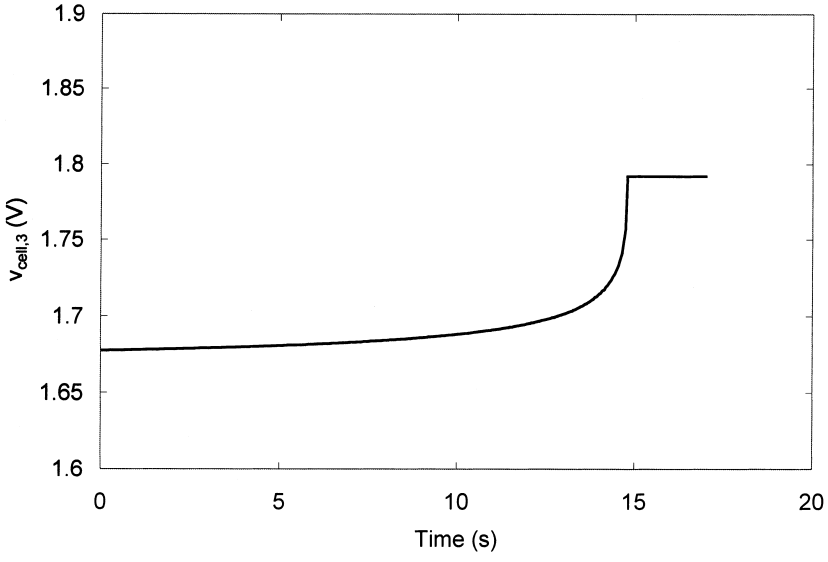

Fig. 7. Predicted voltage of battery 3 in simulation I.

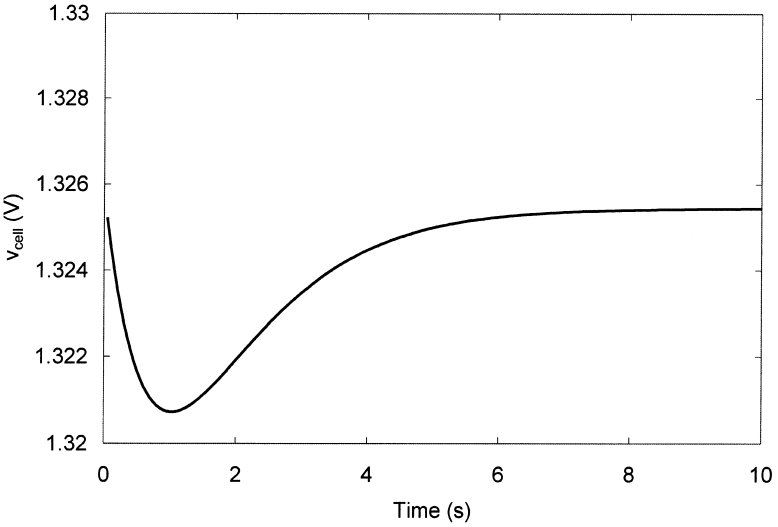

Fig. 9. Predicted voltage of the battery in simulation II.

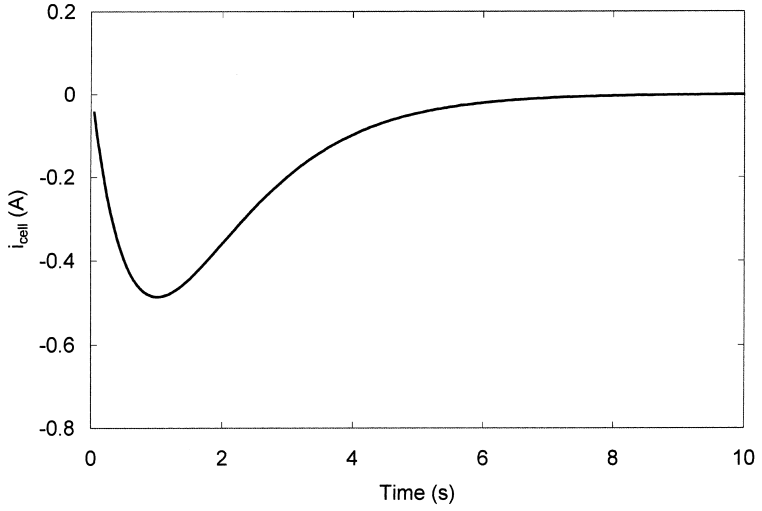

Fig. 10. Predicted current of the battery in simulation II.

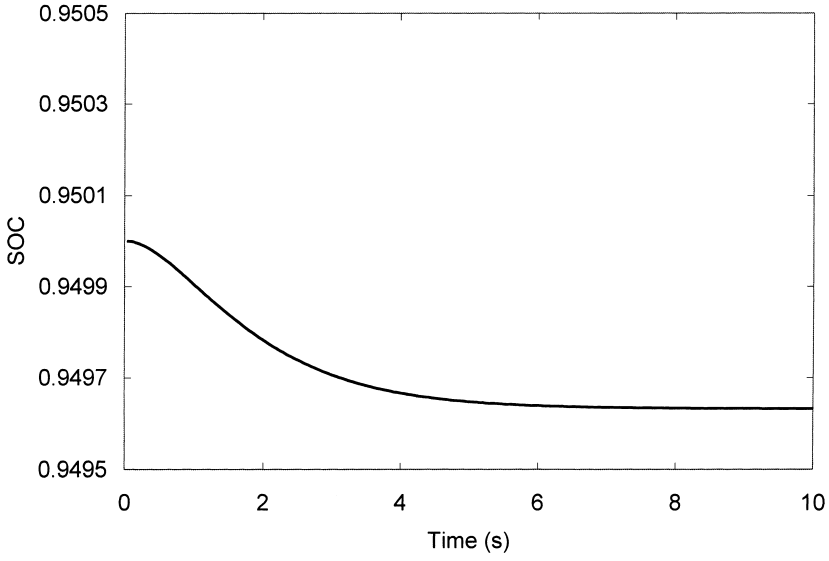

Fig. 11. Predicted SOC of the battery in simulation II.

Table 2
Parameters for the model of a nickel–metal hydride cell

Parameter	Value
a_{pos} (cm^2/cm^3)	4000.0
a_{neg} (cm^2/cm^3)	1000.0
A_{pos} (cm^2)	325.0
A_{neg} (cm^2)	360.0
c_e (mol/cm^3)	7.0×10^{-3}
$c_{e,ref}$ (mol/cm^3)	1.0×10^{-3}
$c_{MH,max}$ (mol/cm^3)	1.0×10^{-1}
$c_{MH,ref}$ ($c_{MH,max}$)	0.5
$c_{Ni(OH)_2,max}$ (mol/cm^3)	3.7×10^{-2}
$c_{Ni(OH)_2,ref}$ ($c_{Ni(OH)_2,max}$)	0.5
$i_{o,1}$ (A/cm^2)	1.0×10^{-4}
$i_{o,2}$ (A/cm^2)	1.0×10^{-10}
$i_{o,3}$ (A/cm^2)	3.8×10^{-4}
$i_{o,4}$ (A/cm^2)	1.0×10^{-4}
l_{pos} (cm)	3.3×10^{-2}
l_{neg} (cm)	2.8×10^{-2}
$L_{Ni(OH)_2}$ (g/cm^2)	6.8×10^{-2}
L_{MH} (g/cm^2)	1.13×10^{-1}
$M_{Ni(OH)_2}$ (g/mol)	92.71
M_{MH} (g/mol)	70.58
$p^0_{O_2}$ (atm)	1.0×10^{-2}
$p_{O_2,ref}$ (atm)	1.0
R_{int} (Ω)	1.0×10^{-3}
SOC^0	0.95
Δt (s)	1.0×10^{-1}
T (K)	298.15
$U_{eq,1,ref}$ (V)	0.527
$U_{eq,2,ref}$ (V)	0.4011
$U_{eq,3,ref}$ (V)	−0.8279
V_{gas} (cm^3)	1.0×10^{-1}
$\rho_{Ni(OH)_2}$ (g/cm^3)	3.4
ρ_{MH} (g/cm^3)	7.49

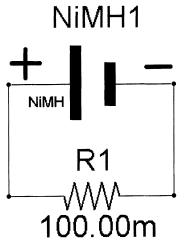

Fig. 13. Worksheet of sample simulation III: a nickel–metal hydride cell with initial SOC of 95% discharges through a 100 m Ω resistor.

Two simulations are provided for the RC model of a nickel–metal hydride cell. The parameters of the nickel–metal hydride cell model are listed in Table 2. The parameters used as the 'old' variables for the initial conditions are shown with a superscript '0' in Table 2. Fig. 12 shows the parameter dialog for the model in VTB. In Fig. 13, a nickel–metal hydride cell with an initial SOC of 95% is connected with a constant resistor of 100 m Ω. The simulated current in circuit is shown in Fig. 14. It is observed that with the drain of SOC of the nickel–metal hydride cell, the current in the circuit gradually decreases, and at the end of the discharge process, the current drops rapidly to zero. Since the cell is connected to a constant resistor, the cell voltage curve similar to Fig. 14 can be expected.

The simulated SOC and hydrogen concentration in the metal hydride electrode are shown in Figs. 15 and 16, respectively. Approximately constant depletion rate of the cell capacity is predicted. It is shown that only half of metal hydride active material is utilized, which is

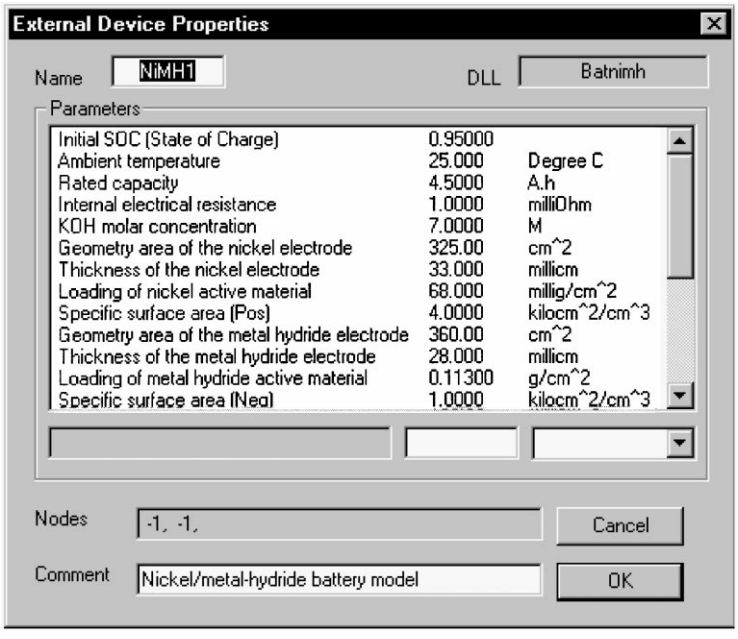

Fig. 12. The parameter setting dialog for the nickel–metal hydride cell model.

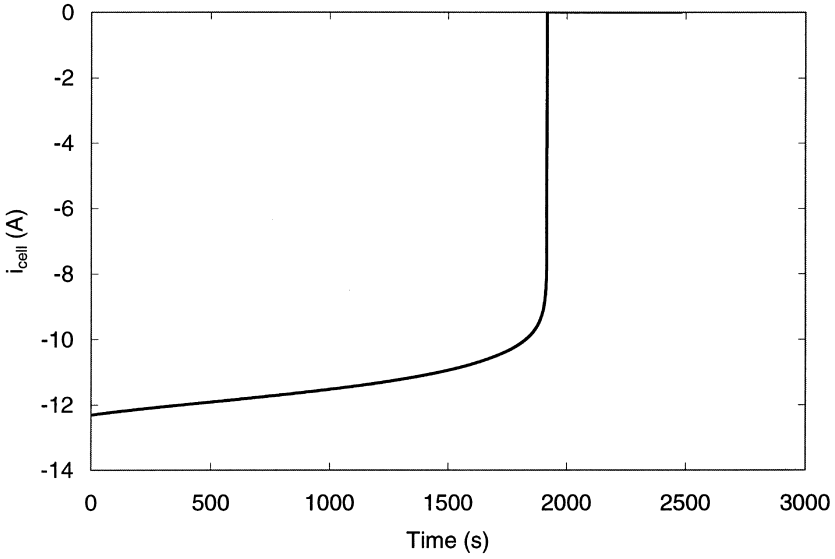

Fig. 14. Predicted current of the cell in simulation III.

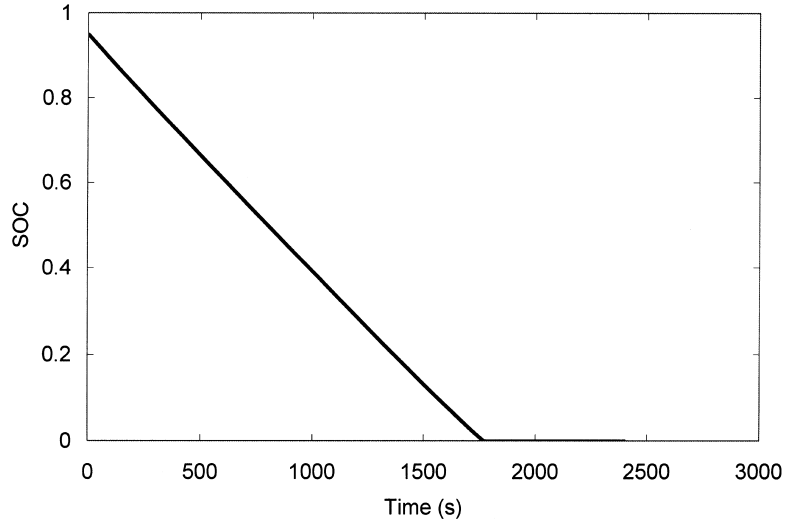

Fig. 15. Predicted SOC of the cell in simulation III.

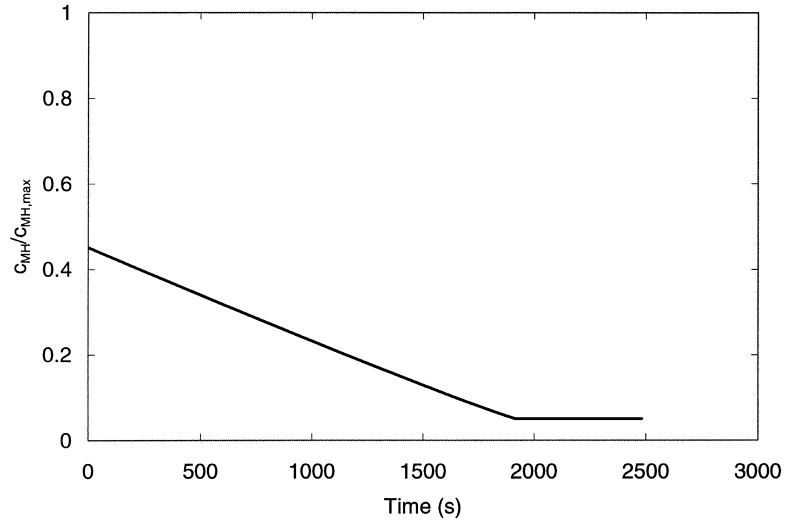

Fig. 16. Predicted mol fraction of hydrogen on the metal hydride electrode of the cell in simulation III.

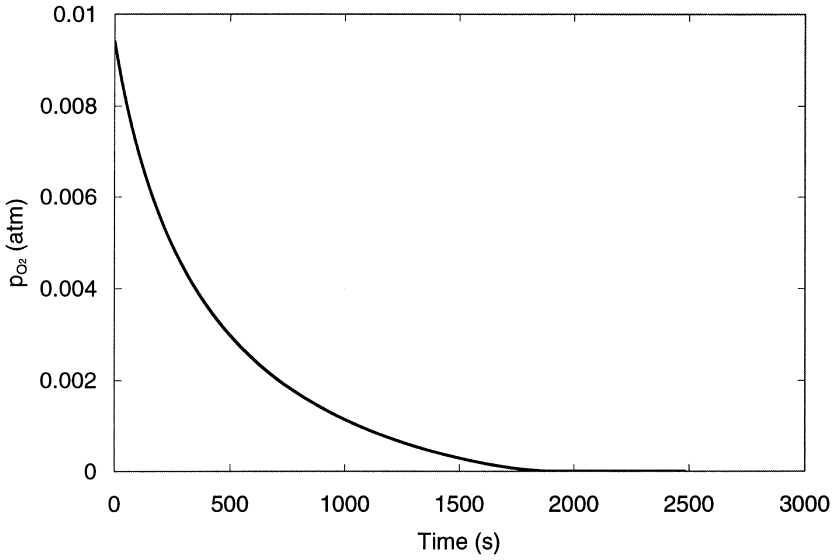

Fig. 17. Predicted oxygen pressure of the cell in simulation III.

consistent with the positive-limited design of the battery. The predicted oxygen pressure in the nickel–metal hydride cell is given in Fig. 17. It indicates that the oxygen pressure decreases gradually with discharge time. As shown in Fig. 18, the potential difference at the solid–liquid interface on the positive nickel electrode gradually decreases at first, and at the end of the discharge process, it changes rapidly to a negative value. In Fig. 19, however, it is shown that the potential difference at the solid–liquid interface on the negative metal hydride electrode only slightly changes during the whole discharge process. It is observed that at the end of the discharge process, the potential difference at the solid–liquid interface on the positive electrode is equal to that on the negative electrode and causes zero current across the cell (and whole circuit).

A simulation involving two nickel–metal hydride cells is shown in Fig. 20. The initial SOCs of two cells are set to be different. The initial SOC of the first one is 95% and that of the second one is 75%. The predicted discharge current is shown in Fig. 21. As can be expected, due to the high voltage of two serially connected nickel–metal hydride cells, the current in the circuit almost doubles that with a single nickel–metal hydride cell. The predicted SOCs in two cells are given in Figs. 22 and 23. It is interesting to note that the less charged cell determines the utilization of both cells, i.e.

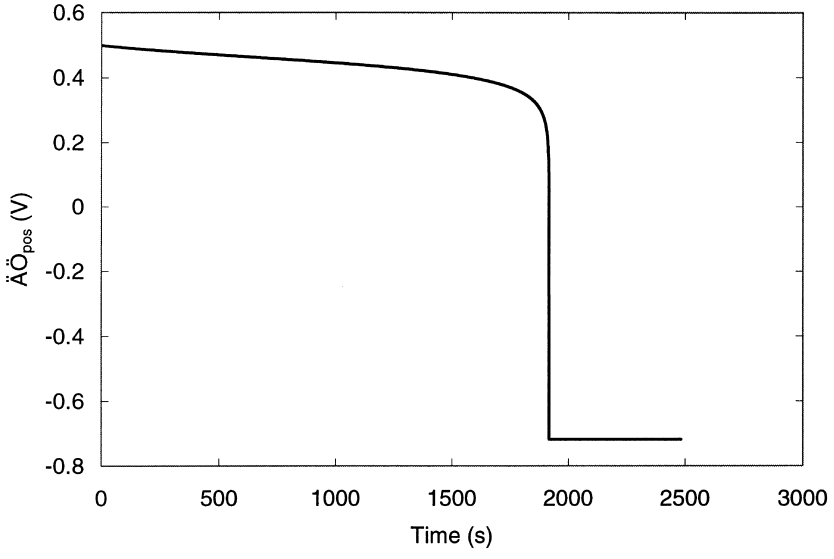

Fig. 18. Predicted potential difference at solid–liquid interface on the nickel electrode of the cell in simulation III.

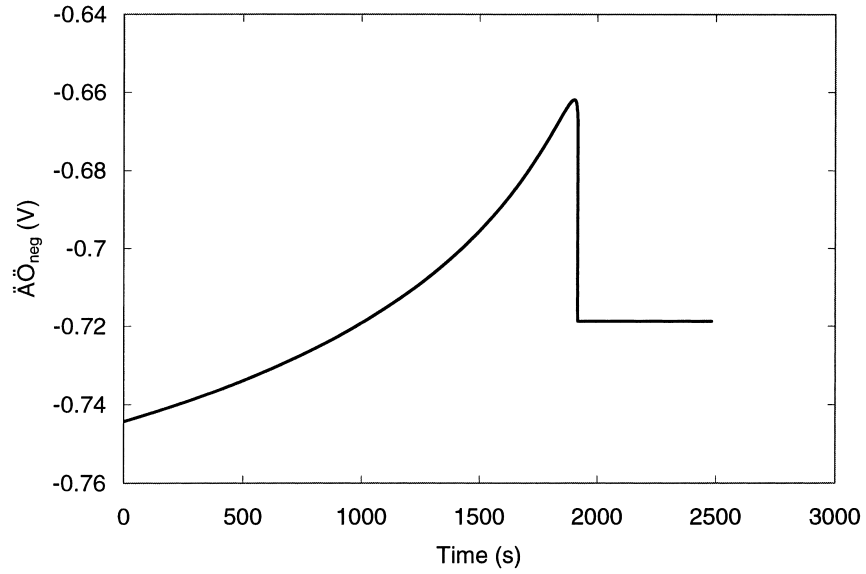

Fig. 19. Predicted potential difference at solid–liquid interface on the metal hydride electrode of the cell in simulation III.

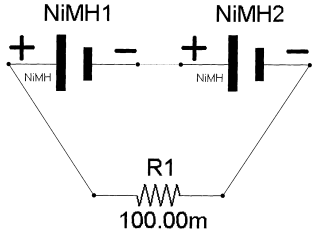

Fig. 20. Worksheet of sample simulation IV: two nickel–metal hydride cells with different initial SOCs discharge through a 100 m Ω resistor.

when the second nickel–metal hydride cell gets fully discharged, it blocks the discharge of the unused capacity of the first cell. Thus, it confirms a common sense in the battery industry, i.e. it is not wise to use two cells with different SOCs.

RC modeling easily allows simulations with multiple objects of the same model, i.e. once a RC model is built, it can be repeatedly used for many objects in a complex system model. This is somewhat different from the conventional battery modeling approach, e.g. if two connected batteries are to be simulated, a more complex model based on the single battery model is required, which is usually a nontrivial task. Usually different objects of the same model may have different parameters, and they are handled simultaneously with the RC solver. It is obvious that challenging battery simulations can be more easily conducted with the RC modeling approach in a simulation environment

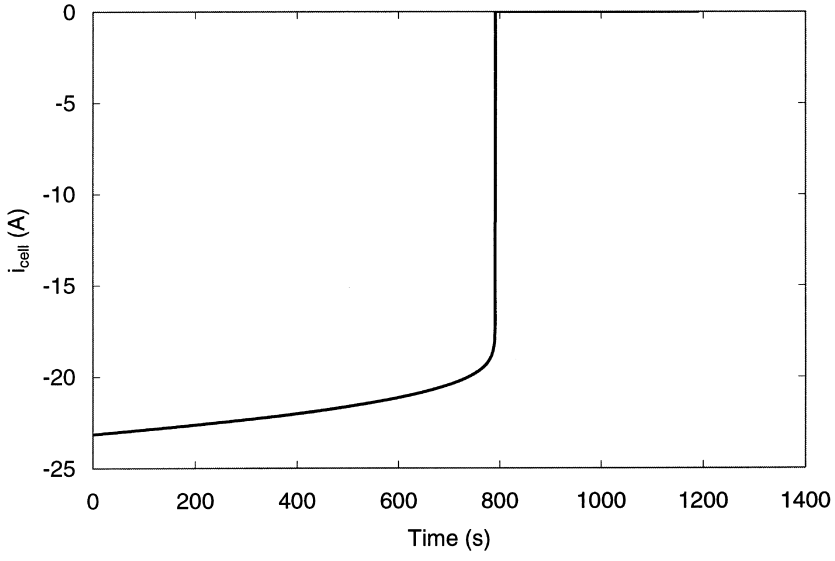

Fig. 21. Predicted current of the cell in simulation IV.

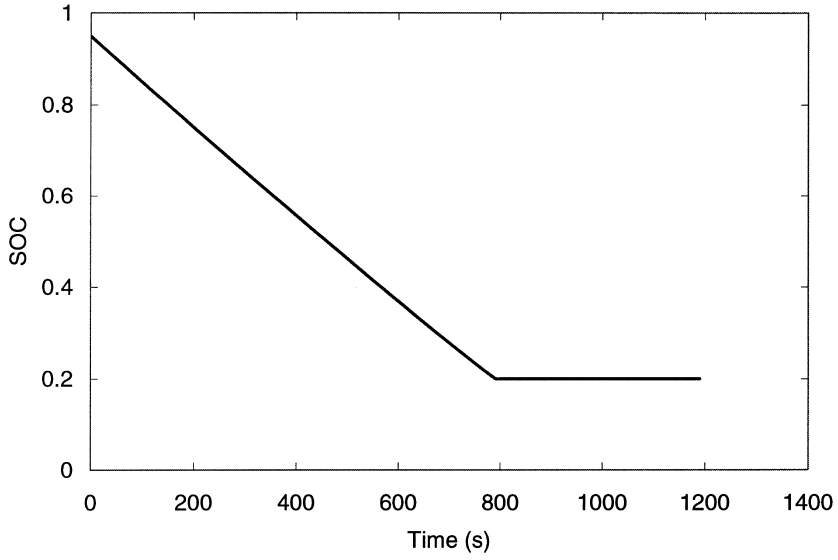

Fig. 22. Predicted SOC of the first nickel–metal hydride cell in simulation IV.

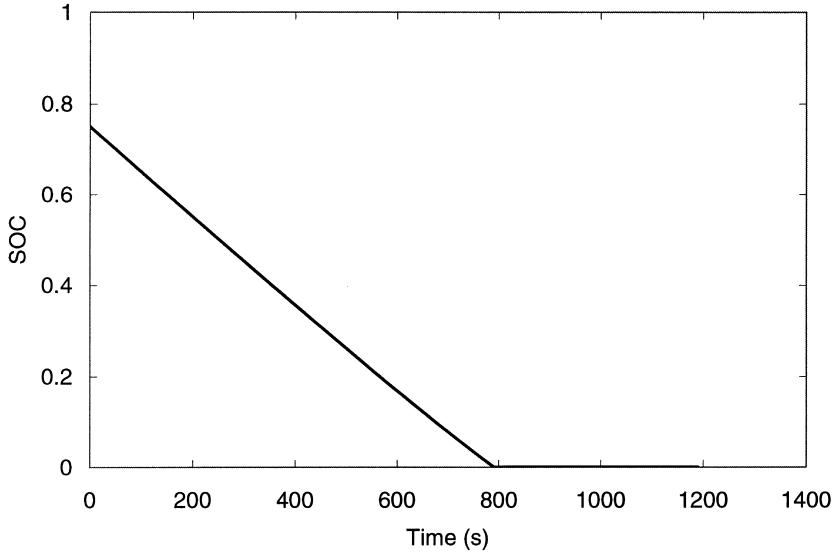

Fig. 23. Predicted SOC of the second nickel–metal hydride cell in simulation IV.

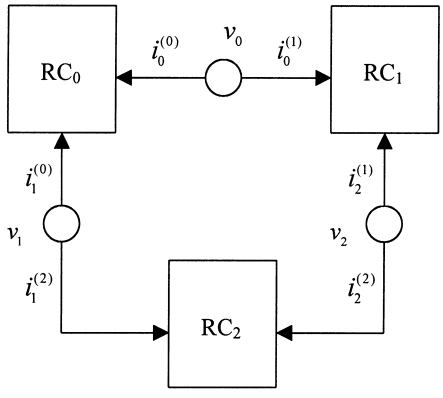

Fig. 24. Schematic diagram of the RC model objects for the worksheet in Fig. 20.

(e.g. in VTB) than with the direct modeling and coding approach.

4. Conclusions

The simulation of interactions among batteries and other electric devices is usually a nontrivial task. In this study, the RC battery modeling for electric circuit simulation is presented. Two RC battery models (a general battery model and a nickel–metal hydride cell model) are demonstrated on the VTB platform. It is shown that challenging simulations involving batteries and other electric devices can be easily handled with the RC modeling approach.

Appendix A. Algorithm of the RC solver in VTB

For an electric circuit system, from the charge conservation and RC model equations, we have the governing equations for the dependent voltage variables $\boldsymbol{v}$ at connecting nodes.

$$\boldsymbol{F}(\boldsymbol{v}) = \sum_{i=1}^{n}(\boldsymbol{g}\boldsymbol{v} + \boldsymbol{b}) = \boldsymbol{0} \tag{A.1}$$

The Jacobian matrix of the above equation with respect to $\boldsymbol{v}$ is given by

$$\boldsymbol{J}(\boldsymbol{v}) = \frac{\mathrm{d}\boldsymbol{F}(\boldsymbol{v})}{\mathrm{d}\boldsymbol{v}} = \sum_{i=1}^{n}\boldsymbol{g} \tag{A.2}$$

The Newton iteration can be used to solve the dependent voltage variables.

$$\boldsymbol{v}^{k+1} = \boldsymbol{v}^{k} - \boldsymbol{J}^{-1}(\boldsymbol{v}^{k})\boldsymbol{F}(\boldsymbol{v}^{k}) \tag{A.3}$$

To get the new iteration values with Eq. (A.3), the inversion of Jacobian matrix is not conducted due to the efficiency and robustness considerations. Instead, $\boldsymbol{LU}$ decomposition procedure is used. First, $\boldsymbol{J}(\boldsymbol{x}^{k})$ is decomposed into upper and lower triangle matrices

$$\boldsymbol{J}(\boldsymbol{v}^{k}) = \boldsymbol{L}\boldsymbol{U} \tag{A.4}$$

Then the following equation is obtained

$$\boldsymbol{L}\boldsymbol{U}(\boldsymbol{v}^{k} - \boldsymbol{v}^{k+1}) = \boldsymbol{F}(\boldsymbol{v}^{k}) \tag{A.5}$$

which can be solved by forward and backward substitution processes, i.e. solve

$$\boldsymbol{L}\boldsymbol{m} = \boldsymbol{F}(\boldsymbol{v}^{k}) \tag{A.6}$$

for vector $\boldsymbol{m}$, then solve

$$\boldsymbol{U}(\boldsymbol{v}^{k} - \boldsymbol{v}^{k+1}) = \boldsymbol{m} \tag{A.7}$$

for $\boldsymbol{v}^{k} - \boldsymbol{v}^{k+1}$ and finally get $\boldsymbol{v}^{k+1}$.

For example, to solve the circuit of three RC model objects connected together in Fig. 20, we have three dependent variables v_0, v_1 and v_2 (see Fig. 24). The governing equations for them are

$$i_0^{(0)} + i_0^{(1)} = 0 \tag{A.8}$$

$$i_1^{(0)} + i_1^{(2)} = 0 \tag{A.9}$$

$$i_2^{(1)} + i_2^{(2)} = 0 \tag{A.10}$$

The RC modeling gives

$$\begin{bmatrix} i_0^{(0)} \\ i_1^{(0)} \end{bmatrix} = \begin{bmatrix} g_{00}^{(0)} & -g_{01}^{(0)} \\ -g_{10}^{(0)} & g_{11}^{(0)} \end{bmatrix} \begin{bmatrix} v_0 \\ v_1 \end{bmatrix} - \begin{bmatrix} b_0^{(0)} \\ -b_1^{(0)} \end{bmatrix} \tag{A.11}$$

$$\begin{bmatrix} i_0^{(1)} \\ i_2^{(1)} \end{bmatrix} = \begin{bmatrix} g_{00}^{(1)} & -g_{01}^{(1)} \\ -g_{10}^{(1)} & g_{11}^{(1)} \end{bmatrix} \begin{bmatrix} v_0 \\ v_2 \end{bmatrix} - \begin{bmatrix} b_0^{(1)} \\ -b_1^{(1)} \end{bmatrix} \tag{A.12}$$

$$\begin{bmatrix} i_1^{(2)} \\ i_2^{(2)} \end{bmatrix} = \begin{bmatrix} g_{00}^{(2)} & -g_{01}^{(2)} \\ -g_{10}^{(2)} & g_{11}^{(2)} \end{bmatrix} \begin{bmatrix} v_1 \\ v_2 \end{bmatrix} - \begin{bmatrix} b_0^{(2)} \\ -b_1^{(2)} \end{bmatrix} \tag{A.13}$$

Substitution of Eqs. (A.11)–(A.13) into Eqs. (A.8)–(A.10) yields

$$\begin{bmatrix} g_{00}^{(0)} + g_{00}^{(1)} & -g_{01}^{(0)} & -g_{01}^{(1)} \\ -g_{10}^{(0)} & g_{11}^{(0)} + g_{00}^{(2)} & -g_{01}^{(2)} \\ -g_{10}^{(1)} & -g_{10}^{(2)} & g_{11}^{(1)} + g_{11}^{(2)} \end{bmatrix} \begin{bmatrix} v_0 \\ v_1 \\ v_2 \end{bmatrix} - \begin{bmatrix} b_0^{(0)} + b_0^{(1)} \\ -b_1^{(0)} + b_0^{(2)} \\ -b_1^{(1)} - b_1^{(2)} \end{bmatrix} = \begin{bmatrix} 0 \\ 0 \\ 0 \end{bmatrix} \tag{A.14}$$

It is obvious that as long as the RC parameters are provided by RC models, the values of v_0, v_1 and v_2 can be easily solved from Eq. (A.14). More complex electric circuits can be solved in the same way. The construction of the governing equations like Eq. (A.14) of the whole simulated system is automatically handled by VTB.

References

[1] J.S. Newman, Electrochemical Systems, 2nd Edition, Prentice-Hall, Englewood Cliffs, NJ, 1991.
[2] P.W. Tuinenga, Spice: A Guide to Circuit Simulation and Analysis Using Pspice, 3rd Edition, Prentice-Hall, Englewood Cliffs, NJ, 1991.
[3] G. Cokkinides, B. Beker, RC and AC models in the VTB time domain solver, Department of Electrical and Computer Engineering, University of South Carolina, 1998.
[4] B. Wu, R.E. White, Comput. Chem. Eng. (2000), in press.